Efficiency of COVID-19 mobile contact tracing containment by measuring time-dependent doubling time

Physical Biology

PAPER

Efficiency of COVID-19 mobile contact tracing containment by measuring time-dependent doubling time

RECEIVED
19 May 2020

REVISED
22 July 2020

ACCEPTED FOR PUBLICATION
4 August 2020

PUBLISHED
6 October 2020

Antonio Bianconi[1,2,3,*], **Augusto Marcelli**[1,4], **Gaetano Campi**[1,2] and **Andrea Perali**[1,5]

[1] Rome International Centre Materials Science Superstripes RICMASS, via dei Sabelli 119A, 00185 Rome, Italy
[2] Institute of Crystallography, CNR, via Salaria Km 29. 300, Monterotondo Stazione, Roma I-00016, Italy
[3] National Research Nuclear University MEPhI (Moscow Engineering Physics Institute), 115409 Moscow, Russia
[4] INFN—Laboratori Nazionali di Frascati, 00044 Frascati (RM), Italy
[5] School of Pharmacy, Physics Unit, University of Camerino, 62032 Camerino (MC), Italy
[*] Author to whom any correspondence should be addressed.

E-mail: antonio.bianconi@ricmass.eu, gaetano.campi@ic.cnr.it, augusto.marcelli@lnf.infn.it and andrea.perali@unicam.it

Keywords: COVID-19, control, mobile tracing, epidemics, SARS-CoV-2, containment measures, efficiency of control policies

Abstract

The COVID-19 epidemic of the novel coronavirus (severe acute respiratory syndrome SARS-CoV-2) has spread around the world. While different containment policies using non-pharmaceutical interventions have been applied, their efficiencies are not known quantitatively. We show that the doubling time $T_d(t)$ with the success *s factor*, the characteristic time of the exponential growth of $T_d(t)$ in the arrested regime, is a reliable tool for early predictions of epidemic spread time evolution and provides a quantitative measure of the success of different containment measures. The efficiency of the containment policy *lockdown case finding mobile tracing* (LFT) using mandatory mobile contact tracing is much higher than that of the *lockdown stop and go* policy proposed by the Imperial College team in London. A very low *s* factor was reached by the LFT policy, giving the shortest time width of the positive case curve and the lowest number of fatalities. The LFT policy was able to reduce the number of fatalities by a factor of 100 in the first 100 d of the COVID-19 epidemic, reduce the time width of the COVID-19 pandemic curve by a factor 2.5, and rapidly stop new outbreaks and thereby avoid a second wave to date.

1. Introduction

The diffusion of COVID-19 is a transnational phenomenon involving all continents, with a million positive cases and thousands of deaths as of early April, 2020. Following of the begining of the very fast COVID-19 epidemic in January 2020 in Wuhan [1, 2], it was found that the characteristic time of the exponential growth was very small (about two days) and the characteristic number R_0 of humans infected by one positive case was about $R_0 = 2.3$, which is much larger than the critical value of 1; these findings point to an explosion with possibly millions of people infected in just a few weeks [3].

In the absence of a COVID-19 vaccine and without established therapies, scientists informed policy makers of the urgent need for epidemic containment measures [4, 5] to reduce the expected hundreds of thousands of deaths during the pandemic's peak. Non-pharmaceutical interventions to reduce care need requests below the number of beds available in hospitals have been proposed for the USA [6, 7] based on experience with containing severe acute respiratory syndrome (SARS). Fast containment measures, such as self-isolation, were included in these proposed interventions. The lockdown stop and go (LSG) protocol was proposed by the Ferguson group of Imperial College [8] based on simulations with models developed on the basis of the influenza pandemic [9, 10]. The epidemic control measures look for a reduction in the number of daily new cases $N(t)$ to avoid an unacceptable load on health care systems and hence reduce the number of deaths. The traditional method to reduce the number of deaths was a lockdown, an emergency protocol that is enforced to prevent people from leaving a given area, city, or region. This containment measure expands the time lapse of the virus' diffusion by stretching the expo-

nent of its exponential growth. Therefore, while the number of cases will decrease at the top, the duration of the epidemic will extend; moreover, this will be accompanied by a severe negative impact on the economy.

China first focused on an unconventional COVID-19 policy to reduce both the number of deaths and the duration of the epidemic [1]. This unconventional policy, called here *lockdown, case finding, mobile tracing* (LFT), was based on a combination of measures looking to reduce both the number of new daily cases at the epidemic's peak and to reduce the time width of the epidemic curve. By reducing both the maximum height and width of the diffusion peak, China obtained a drastic reduction in the total number of deaths. After about 80 d from when the epidemic threshold was excedeed, on April 7th 2020 China's long-term lockdown was stopped, with officially less than 3400 fatalities. This was the largest 'experiment' to test the efficiency of the new LFT policy in the history of epidemiology, and it took advantage of both a mass search of positive cases and tracing of infected cases through a mobile phone application. A similar approach has been considered by other countries, taking advantage of software applications designed to run on mobile phones and treatments of Big Data developed in recent years. The success of the Chinese and South Korean COVID-19 policies was considered by other countries such as Norway, Singapore, and Taiwan as they developed their own approaches [5].

The more conventional approach—a type of '*herd immunity*'—has been considered by European countries and the USA. It is called *lockdown stop and go* LSG, [8]. The LSG approach is made up of a combination of advice for the population to keep '*physical distance*' to protect others, for only positive cases to stay at home, for family members of a positive case to adopt a household quarantine, and to reduce travel. Intermittent measures are planned to be temporarily relaxed for short time windows, and reintroduced when positive case numbers rebound [8]. The media informed the population about the actual numbers of epidemic cases, and the advisories diffused only weeks after the COVID-19 pandemic onset.

Italy, France, and Spain first followed the LSG policy, and in March 2020 employed the mitigation strategy called here *mandatory full lockdown* (MFL); there were a few days of delay in fully adopting the MFL, during which the LSG approach was strongly enforced. These unprecedented measures of imposition by law all over the country consisted of enforcing physical distancing; ordering closure of schools, universities, and all national manufactures; a ban of mass gatherings and public events; and confinement at home of the entire population. This approach had the key target of reducing the number of infected cases per day and being careful not to overcome the maximum number of sick persons requiring critical care [6–8]. The MFL policy gives priority to the health care system with respect to other economic demands.

An academic epidemiology analysis is usually made at the conclusion of an epidemic. However, in the case of the COVID-19 pandemic, some countries immediately shared verified data and made them available in public repositories. This opportunity gives scientists the possibility to shed light on the new physics of epidemics with containment measures [11–19], which is becoming a field of high interest in relation to populations, health systems [8, 9], travel industries [20, 21], and the economy [10]. This is a highly interdisciplinary research area, at the intersection among biological physics, advanced statistical physics of complex systems, physics of quantum complex materials, chain reactions control in nuclear reactors, and the most recent Big Data analysis methods.

It is clear that in the early days COVID-19 followed the classical exponential law of epidemic spread with a constant rate, but a few scientists [11–19] realized that this was followed by a second regime with a variable time-dependent rate that was quite different across countries applying different policies. However, in spite of the relevance of the question, no one was able to measure in a quantitative way the relative efficiency of the different containment measures based on verified COVID-19 data released by official institutions and health agencies; this is key information needed to stop this pandemic.

Only two weeks after the start of the MFL policy, it was [13, 14] pointed out that the slowing down of the pandemic's diffusion was much less effective with the MLF approach than with the LFT approach. The data analysis approach [13, 14] used the quantitative determination of the time-dependent doubling time $T_d(t)$ of the COVID-19 pandemic spread calculated by averaging *day by day* data over a five-day interval. The measure of the time-dependent doubling time (T_d) is widely used not only in epidemiology but also in nuclear reactor physics, where it is used to keep the reactor in the critical regime between the subcritical regime of the chain reactions of nuclear fission processes and the supercritical regime with risks of severe explosive accidents. The similarity of the nuclear chain reactions in uranium with biological cell fission was noticed by Lise Meitner and Otto Robert Frisch when they coined the term 'nuclear fission' in 1939.

The comparative analysis of the time-dependent doubling time data from South Korea and Italy on March 15th after about 20 d from the epidemic threshold t_0 shows that the LFT-controlled COVID-19 growth entered the arrested phase in South Korea while in Italy it was still rapidly growing in the near threshold phase [13, 14]. This was possible because the doubling time analysis shows two well-separated regimes: the first near threshold phase is described by a stretching exponential with a slowly increasing

stretched characteristic time; this is followed by a second phase, the arrested growth process following the Ostwald growth over time, where one phase transforms into another metastable phase, but with a similar free energy [13, 14, 22–24]. This mechanism has been observed in the diffusion of oxygen interstitials diffusion in quantum complex matter [25–27] and in the crystallization of complex molecules [28] and proteins [29].

2. Results and discussion

The different efficacies of the containment policies are presented in figure 1(a), where the cumulative number of cases $N_c(t)$ in different countries deposited in data banks on the 95th day of the year (DoY) is plotted against the time scale, with zero set as the first day t_0 of the exponential growth. The time t_0 of the epidemic threshold is defined as the day when the time-dependent doubling time shows a minimum before it starts to increase. Using this criterion, the cumulative number of cases shown in figure 1(a) follows an average exponential law from the 5th to the 14th day with a doubling time of about three days and about 60 cases at the initial time t_0 of the epidemic threshold.

As can be seen in panel (a) of figure 1, the diffusion rate in various countries with different policies is similar in the near threshold regime. Indeed, the reported curves of the cumulative number of cases $N_c(T)$ overlap in the near threshold regime during the first days while they strongly diverge in the arrested regime. The positive case curves in the USA and UK were predicted [7, 8] using the standard individual-based simulation model developed to support pandemic influenza planning [9, 10]; these curves are plotted in panels (b) and (c). The calculated time-dependent number of hospital beds dedicated to intensive care medicine for the case of wild uncontrolled epidemic in panel (b) implies the failure of both USA and UK health care systems [6–8]. To avoid the break down, it was proposed to reduce the peak intensity in panel (b) by expanding the epidemic time scale by a factor 1.5 using non-pharmaceutical interventions, e.g., case isolation, home quarantine, and physical distancing, as evident in panel (c). In this work, in order to evaluate the time evolution of the epidemic growth, we used the time-dependent doubling time $T_d(t)$ as the key physical parameter:

$$T_d(t) = \frac{\ln(2)}{\frac{d[\ln(N_c(t))]}{dt}}, \quad (1)$$

where $N_c(t)$ is the cumulative number of cases, and the derivative at each time t is obtained by averaging the $N_c(t)$ curve over a period of five days.

The efficacy of the containment policies is probed by the increase in $T_d(t)$ from its minimum value $T_{d0} = 2$ d, at the time threshold t_0, to time t^* where $T_d = 50$d. This value of the doubling time is where the exponential growth in the supercritical phase ($T_d < 50$) is expected to stop because it is the lowest limit of the COVID-19 epidemic critical phase; it is in the range $50 < T_d < 100$ d, and the reproduction number R_0 is near one [30]. Therefore, we calculated $T_d(t)$ curves in panels (b) and (c) of figure 1; they show the exponential increase in $T_d(t)$ in the time range of the exponential growth [13, 14]. A kink in $T_d(t)$ separates two exponential increasing regimes: the near threshold regime (shaded blue region) and the arrested regime (shaded yellow region). These regimes are separated by the transition regime around the peak number of new daily cases $N(t)$. The theoretical curves of $T_d(t)$ for the uncontrolled epidemic (black filled dots in panel (b)) and those with the lockdown mitigation (blue filled dots) illustrate changes in the time evolution behavior, which depends on the containment policy. First, in the near threshold regime, the doubling time follows an exponential growth (blue line in the semi-log scale) with the characteristic time s_1

$$T_{d1} = C_1\ e^{t/s_1} \quad (2)$$

and in the arrested regime it follows a second exponential growth (red line in the semi-log scale) with the characteristic time s_2

$$T_{d2} = C_2\ e^{t/s_2}. \quad (3)$$

The figure shows that the theory predicts that s_2 is much smaller than the characteristic time s_1. In fact, by measuring the average $\langle s \rangle$ factor by fitting the full $T_d(t)$ curve in the range $2 < T_d < 50$ [13, 14], we quantitatively measured the efficiency and effectiveness of the enforced containment policy in terms of time. The extraction of $\langle s \rangle$, s_1, and s_2 factors allows a straightforward quantitative evaluation, and a quantitative comparison of the different containment policies adopted to control the epidemic becomes possible. The calculations show that the factor s_1 decreases in the near threshold regime from the wild regime value $s_1 = 80$ d (panel (b)) to the lockdown regime $s_1 = 140$ d (panel (c)). Meanwhile, factor s_2 in the arrested regime increases from the wild regime value $s_2 = 8.2$ d (panel (b)) to the lockdown regime $s_2 = 14.2$ d (panel (c)).

The doubling time $T_d(t)$ reaches 50 d after more than two months in the wild uncontrolled pandemic spread curve. Conversely, this value is reached after 110 d in the most severe lockdown policy, i.e., the pandemic is predicted to be about 1.6 times longer in the lockdown regime, which is in agreement with the ratio of the half width values at half maximum.

The explosion of the COVID-19 pandemic resulted in a fast response of the scientific community proposing different models to test containment measures; these models can be quickly verified or falsified by analyzing experimental data [11–19].

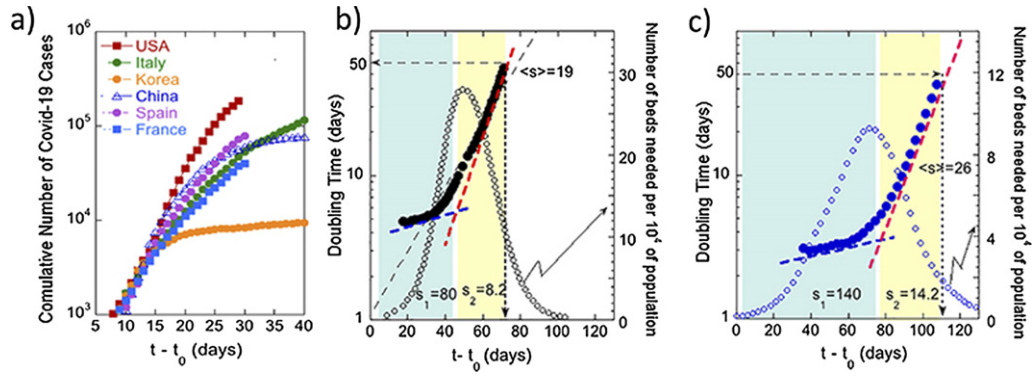

Figure 1. Standard curves used to report the COVID-19 epidemic time evolution showing the cumulative number of cases (panel (a)) and the standard theoretical epidemiology predictions of the needed number of beds based on the prediction of daily new cases for an uncontrolled epidemic case (panel (b)) and a mitigated epidemic case (panel (c)). Panel (a) shows the cumulative number of positive cases $N_c(t)$ vs time in South Korea (orange), France (blue), China (light blue), Italy (green), Spain (magenta), and the USA (red). The time scale for each curve of each country starts on the threshold day t_0. The curves overlap in the near threshold regime and later separate. The curves of the cumulative number of cases in China and South Korea become flat after about 30 d, when the pandemic is arrested. Panels (b) and (c) present the theoretical predictions for the number of needed intensive care units (open symbols) from [8] for an uncontrolled diffusion (b) and for severe containment measures (c). We show in panel (b) our calculation of the exponential variation of the doubling time $T_d(t)$. The time-dependent doubling time curves calculated in this work are for an uncontrolled (black curve in panel (b)) and controlled epidemic (blue curve in panel (c)). Our calculations predict a different exponential increase in the doubling time in the near threshold regime (blue area) and in the arrested regime (yellow area). The stop of the positive case curve occurs in the range of $50 < T_d(t) < 70$ d where the reproduction number $R(t)$ becomes less than one, and the critical regime is entered, where the effective infection time becomes equal to the effective removal time.

The key results of our work are shown in figures 2 and 3 where we report the doubling time $T_d(t)$ as a function of time, extracted by verified data vs time with the zero set at the threshold time t_0 in several countries where different COVID-19 epidemic policies were enforced. The time evolution of the experimental doubling time $T_d(t)$ for South Korea and China, where the LFT policy was applied, is plotted in panel (a). The positive case curves are constructed of verified data of the number of daily new cases $N(t)$. The experimental doubling time $T_d(t)$ where the time unit is one day is calculated using equation (1) and does not need any normalization. In South Korea, after the threshold of the epidemic outbreak is reached, $T_d(t)$ increases exponentially up to time t^* where $T_d(t)$ reaches 50 d. For $t > t^*$, $T_d(t)$ remains constant, hence showing the transition from exponential to linear growth. In our investigation of the COVID-19 outbreak in Italian regions [30] we extracted both the time-dependent reproduction number $R(t)$ and the doubling time $T_d(t)$, showing that the critical phase where $R_t \approx 1$ corresponds with the doubling time fluctuating in the range $50 < T_d(t) < 100$. This regime separates the exponential growth phase (called the supercritical phase), with $R_t > 1$, from the phase with $R_t < 1$ (called the subcritical phase). Therefore, the time width of the exponential growth regime giving the characteristic width of the COVID-19 positive case curve can be measured by the difference between day T^*, where T_d reaches 50 days, and the outbreak threshold time t_0. We found that the full time width is 27 d for China and 24 d for South Korea. Through introducing a normalized scale, i.e., dividing the time in the time axis by the full time width, both the normalized curves of $N(t)$ and the experimental $T_d(t)$ curves for China and South Korea fully overlap, thereby providing evidence for the characteristic behavior associated with the mandatory 'contact tracing' LFT policy.

The key result of the data analysis is that the kink in the $T_d(t)$ curves, which separates the near threshold regime from the arrested regime, is only 13–14 d. The different value of the s_1 factor in the near threshold regime is due to the immediate activation of the LFT policy with mandatory mobile contact tracing as requested by scientists and experts [3, 4]. This was adopted by policy makers in South Korea faster than in China.

The overlapping positive case curves of these countries also shows that both the epidemic peak and its full time width at half maximum are strongly reduced by the LFT policy with mandatory 'contact tracing'. In table 1 we report the key parameters obtained by the fits to unveil the physics of the time evolution of the pandemic in the selected countries.

Panel (b) of figure 2 shows that the time-dependent doubling time $T_d(t)$ in Italy, Spain, and France, where the MFL policy (without the mandatory 'contact tracing' LFT policy) was applied, fully overlap. In the near threshold regime, the values of the doubling time are very similar and the three curves show the same kink: the transition from the near threshold to the arrested regime occurs at 27 d. This value was used to normalize the time scale. On the 102nd DoY, the arrested regime in these countries was only at its early stage with the same factors.

The time-dependent doubling time for the USA

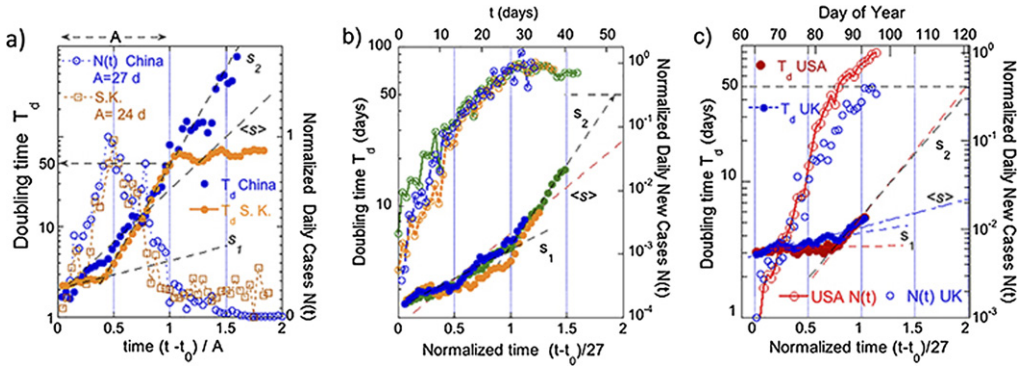

Figure 2. In this figure we report the time evolution of the doubling time T_d, which we propose here to shed light on the unconventional time evolution of the COVID-19 pandemic with containment measures. Panel (a) depicts the evolution of the experimental doubling time $T_d(t)$ in the countries where the LFT policy was enforced: South Korea (filled orange dots) and China (filled blue dots). The open circles are the known data of the number of daily new cases $N(t)$, and are used here to track the time evolution. Panel (b) presents the experimental time-dependent doubling time $T_d(t)$ in Spain (filled orange dots), France (filled blue dots), and Italy (filled blue dots), where the MFL policy was applied. Panel (c) presents the evolution of the doubling time in the USA (filled red dots) and the UK (filled blue dots), which applied the LSG policy. The $N(t)$ curves are plotted in semi-log scale in panels (b) and (c). In panels (a) and (b) the numbers in the $N(t)$ curves are normalized to overlap all curves in the near threshold region. The near threshold time regime in panels (b) and (c) identified in the range between the threshold and the kink in the $T_d(t)$ is 27 d in panel (b) and similar in panel (c).

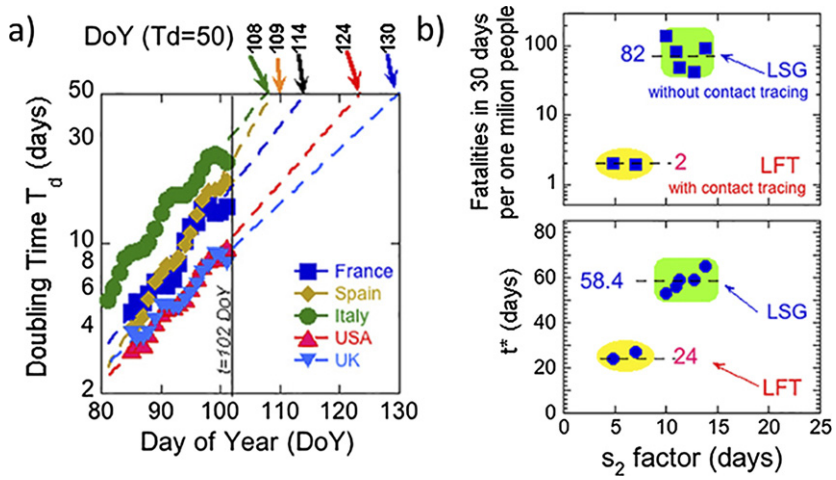

Figure 3. Extrapolated time T^* of the DoY when the doubling time T_d will reach 50 d, $T_d(T^*) = 50$, used to predict the time width of the supercritical epidemic regime $t^* = T^* - t_0$ for LSG countries. Data is that available on the 102nd DoY. The quantitative test of the efficiency of one containment policy versus another is given by (i) its ability to achieve a short time width t^* and (ii) to reduce the number of fatalities in the same time period normalized to the population. Panel (a) plots the doubling time $T_d(t)$ as a function of time in the arrested regime for the epidemic spread in Italy, France, Spain, the UK, and the USA. The linear fit in the semi-log scale allows the prediction of the expected day T^* of the year when T_d will be 50. The predicted time duration of the supercritical regime is given by $t^* = T^* - t_0$. Panel (b) plots t^* as a function of the success factor s_2. The lower panel shows that both s_2 and t^* are smaller in the LFT countries (data in the yellow area) than in LSG countries (data in the blue area). The average value $t^* = 24.8$ d in countries where the LFT protocol was enforced is about a factor of 2 lower than the average value $t^* = 58.4$ d in countries where the LSG protocol [8] was followed; this is in agreement with data presented in figure 2(b). The upper panel (b) shows that the normalized number of fatalities in 30 d per million people in the countries that adopted the LSG protocol without mandatory mobile contact tracing are similar among them, and their average of $N_{30} = 82$ is 40 times larger than the $N_{30} = 2$ reached in the countries that adopted the LFT protocol with mandatory mobile contact tracing.

and UK, which later adopted a softer version of the LSG policy, is plotted in panel (c) of figure 2. While scientists and some policymakers asked their governments to activate containment measures as soon as possible [5], for some time USA and UK policymakers chose to 'do nothing'. This had a clear impact on the s_1 factor, as outlined by the flat $T_d(t)$ curve in the near threshold regime; moreover, there is a similar constant behavior between the USA and the UK, with a very large s_1 factor.

Panel (a) of figure 3 plots the exponential increase in the doubling time in the arrested regime for all five investigated countries applying the LSG policy without the mandatory 'contact tracing' policy on the 102nd DoY. From the extrapolation of the line in the semi-log scale (as determined by the exponential curve of $T_d(t)$ in the arrested regime) it is possible to predict the time duration of the supercritical phase and thereby show the exponential growth in these five countries that adopted the LSG policy.

Table 1. The parameters of the time evolution of the COVID-19 pandemic in different countries, calculated from data available on the 102nd DoY 2020. (a) t_0, DoY of the threshold of epidemic national outbreak; (b) doubling time $T_d(3\text{ d})$ at the third day from the threshold; (c) s_1, the s factor in the near threshold regime; (d) s_2, the s factor in the arrested regime; (e) prediction of the DoY T^* when the doubling time $T_d(T^*)$ will reach 50 d; (f) prediction of the time duration $t^* = T^* - t_0$ of the COVID-19 epidemic's exponential growth in the supercritical regime with doubling time $T_d(t^*) < 50$ d; (g) population of each considered country; (h) number of fatalities per million people during the first 30 d of the national outbreak in each country.

Data of 102nd DoY	(a) t_0 outbreak time threshold (DoY)	(b) T_{d3} at 3rd day	(c) s_1 (d)	(d) s_2 (d)	(e) Predicted T_s^* (DoY) when $t_d = 50$ is expected	(f) Predicted $t^* = T^* - t_0$ time interval of the supercritical phase (d)	(g) Population (millions)	(h) Fatalities in the first 30 d per million people
USA	65 ± 1	3 ± 0.2	388	12.7 ± 1	124 ± 2	59 ± 4	328.200	42.563
Italy	52 ± 1	2.5 ± 0.2	30	11 ± 1	108 ± 2	56 ± 4	60.360	84.601
Spain	56 ± 1	2.7 ± 0.2	56.5	10 ± 1	109 ± 2	53 ± 4	49.940	139.03
France	55 ± 1	2.6 ± 0.2	29.5	11.3 ± 1	114 ± 2	59 ± 4	66.990	49.764
UK	65 ± 1	3 ± 0.2	84	13.8 ± 1	130 ± 2	65 ± 4	66.650	94.432
China	22 ± 1	2 ± 0.2	9.4	7 ± 1	49 ± 1	27 ± 2	1393.000	1.9093
South Korea	48 ± 1	2.3 ± 0.2	43	4.8 ± 1	72 ± 1	24 ± 2	51.640	2.0365

The exponential growth is expected to enter the critical regime when the doubling time $T_d(t^*) > 50$ d, as shown for the case of South Korea in figure 1. However, it is not possible to predict how long this critical regime will continue since the number of daily new cases could show either large fluctuations or decrease or increase linearly, as what occurred in South Korea for a long time.

The linear fit of the doubling time in the arrested regime $T_d(t)$ in the semi-log scale shown in panel (a) of figure 3 for the five countries where the LSG policy was enforced (Italy, France, Spain, the UK, and the USA) allows us to predict the expected day T^* of the year when T_d will be 50 (called DoY stop): 108 in Italy, 109 in Spain, 114 in France, 124 in the USA, and 130 in the UK, with an error bar of ∼2 d. The time width t^* of the epidemic curves of these countries is given by the time difference $t^* = T^* - t_0$, which is predicted to be in the range of 55–63 d (see table 1), i.e., it is more than two times longer than for countries where the mandatory 'contact tracing' LFT policy was not adopted. In table 1 we summarize the key numerical results based on data available on April 10th.

In the lower panel of figure 3(b) we report the estimated time width t^* of the COVID-19 epidemic supercritical regime as a function of the s_2 factor. The success factor s_2 in countries that enforced the LFT policy with mandatory 'contact tracing' is in the range of $5 < s_2 < 7$ while the s_2 factor in countries that enforced the LFT policy without mandatory 'contact tracing' falls in the range of $10 < s_2 < 15$.

The time width t^* in the countries that applied the LSG protocol proposed by Imperial College [8] without mandatory contact tracing is predicted to cluster around the average value of 58.4 d in the blue area; this is two times larger than the average value of 24.8 d observed in countries where the LFT protocol was enforced, and is in agreement with the differences in the time widths shown in figure 2.

In order to quantitatively evaluate the efficiency of the different policies in taking care of the health of the population in different countries, it is necessary to calculate the number of fatalities collected over the same time interval and normalize it to the country's total population. On the 102nd DoY, we analyzed all cumulative curves of COVID-19 fatalities of all studied countries in the first 30 d of the epidemic's spread. Therefore, in the upper panel of figure 3(b) we have plotted the number of fatalities in the first 30 d divided by the total population of all studied countries (measured in millions) as a function of the s_2 factor. The data from countries that applied the LFT policy with mandatory mobile tracking [13–15] occur in the yellow region, showing that these countries achieved a both a lower s_2 factor and a lower number of fatalities. The countries in the blue region, using the LSG protocol [8] with no mandatory mobile tracking, achieved an s_2 factor about two times larger. Moreover, on April 10 the average number of normalized fatalities is 40 times higher in all countries using the LSG protocol without mandatory contact tracing than in countries using the LFT protocol with mandatory contact tracing.

3. Validation of predictions and evaluation of containment protocols

On June 25, 2020, in the course of the peer review process of this paper, we were invited to check our results by analyzing new available data on the spread of COVID-19. The data made available on the 177th DoY of 2020 allow us to make a comparative evaluation of the efficiency of LFT and LSG containment protocols in the same time range (100 d, i.e., covering the entire positive case curve); these new data also enable us to validate the accuracy of predictions based on data covering only the first 15 days or the first 30 days [13, 14]. The time evolution of the dou-

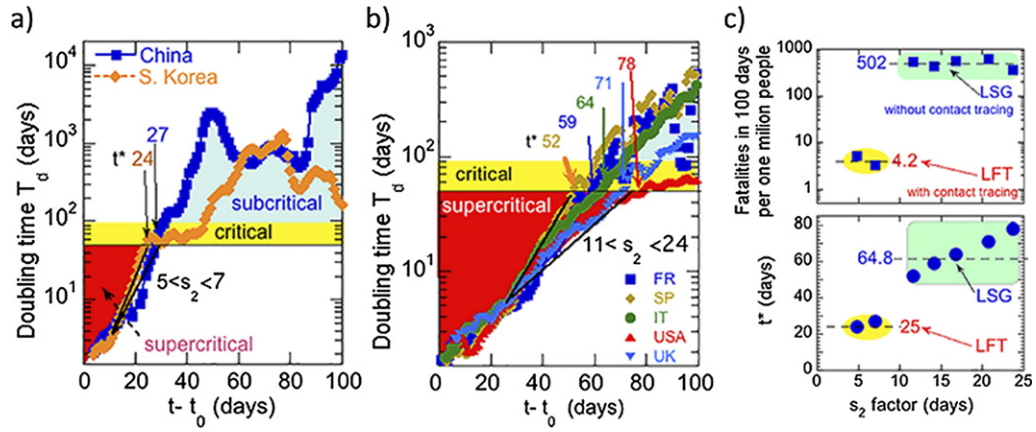

Figure 4. The analysis of data available on the 177th DoY allowed us to measure the time-dependent doubling time $T_d(t)$ in the first 100 d after a national outbreak, covering the full time width of the epidemic curve in the supercritical regime. Panel (a) shows the curves $T_d(t)$ in countries that adopted the LFT protocol with mandatory mobile contact tracing. Panel (b) shows the curves $T_d(t)$ in countries that adopted the LSG protocol without mandatory mobile contact tracing. The supercritical regime is indicated by the red area, and is characterized by exponential growth for $t < t^*$ where $T_d(t) < 50$ d. The time t^* where $T_d(t^*) = 50$ d is assigned to the transition from the supercritical regime to the critical regime (yellow area) occurs in the range of 50 d $< T_d(t) <$ 100 d. The subcritical regime (blue area) occurs where $T_d(t) > 100$ d. The success factor s_2 measured in the supercritical regime is in the range of $11 < s_2 < 24$ in the LSG countries (panel (b)) but is much smaller in the LFT countries (in the range of $5 < s_2 < 7$; see panel (a)). The duration t^* of the supercritical regime is in the range of $52 < t^* < 78$ d, with the average value $\langle t^* \rangle = 64.8$ days in LSG countries (panel (b)). We can compare this with the $24 < t^* < 27$ d in LFT countries. Panel (c) shows the time duration t^* of the supercritical regime (lower panel) and the number of fatalities in the first 100 d per million people (upper panel) as a function of s_2. The lower panel shows that both s_2 and t^* are shorter in the LFT countries (yellow area) than in LSG countries (blue area). The upper panel shows that the normalized average number of fatalities over 100 d is about 129 times higher in countries where the LSG protocol [8] was enforced ($N_{100} = 502$) compared to countries where the LFT protocol was enforced ($N_{100} = 42$).

Table 2. The parameters of the time evolution of the COVID-19 pandemic in different countries calculated from data available on the 177th DoY 2020. (a) The s_2 factor of the exponential growth of the doubling time in the arrested regime of the supercritical phase; (b) the measured DoY T^* when the doubling time $T_d(T^*)$ reached 50 d, i.e., $T_d(T^*) = 50$ d; (c) the measured time interval $t^* = T^* - t_0$ of the supercritical phase where $T_d(t) < 50$ d; (d) number of fatalities per million people (normalized to the country population) during the first 100 d of the national outbreak of each country.

Data collected on 177th DoY	(a) s_2 (d)	(b) T^* measured time (DoY) when $t_d = 50$	(c) Measured $t^* = T^* - t_0$ time interval of the supercritical phase (d)	(d) Fatalities in the first 100 d per million people
USA	23.7 ± 1	143 ± 1	78 ± 2	357.55
Italy	16.8 ± 1	116 ± 1	64 ± 2	552.60
Spain	11.6 ± 1	108 ± 1	52 ± 2	543.37
France	14.1 ± 1	114 ± 1	59 ± 2	436.55
UK	20.7 ± 1	136 ± 1	71 ± 2	623.72
China	7 ± 1	49 ± 1	27 ± 2	3.3288
South Korea	$4, 8 \pm 1$	72 ± 1	24 ± 2	5.2285

bling time in the first 100 d from the outbreak time threshold are shown in panel (a) of figure 4 for countries following the LFT protocol and in panel (b) of figure 4 for countries following the LSG protocol. The supercritical phase, characterized by the exponential growth of the epidemic, which occurs for $t < t^*$ where $T_d(t) < 50$ d [30], is indicated by the red area. The yellow area, where $50 < T_d(t) < 100$ d, indicates the critical regime. The time duration of the supercritical phase is much shorter for LFT countries than in LSG countries, i.e., $24 < t^* < 27$ d (panel (a)) vs. $52 < t^* < 78$ d (panel (b)), respectively. The time width of the supercritical regime is much longer than predicted in figure 3 for the UK and USA The success s_2 factor, measured in the supercritical regime for the LSG countries, is in the range of $11 < s_2 < 24$ (see the blue area of panel (b)). It is larger than predicted in figure 3 and is much higher than in the LFT countries, where s_2 is in the range of $5 < s_2 < 7$ (panel (a)).

On the 177th DoY it was possible to analyze the cumulative curves of COVID-19 fatalities of all studied countries over the same interval of 100 d, thus covering the full width of the epidemic wave. The impact of different containment policies on the population was measured by the relation between the number of fatalities in the first 100 d per million people (N_{100}) and the s_2 factor shown in panel (c) of figure 4. The s_2 factors and the number of fatalities N_{100} are reported in table 2.

Qualitative predictions made in [13, 14] and predictions made on April 10 (see panel (b) in figure 3) are confirmed. The upper panel of figure 4(c) shows the number of fatalities (N_{100}) in the first 100 d per million people as a function of s_2. The results based on data collected on June 25 in panel (c) of figure 4 qualitatively confirm the predictions made on March 15 [14, 15] and April 10, which are shown in panel (c) of figure 3. All results confirm that a lower s factor is correlated with both a short duration of the supercritical epidemic regime and a lower number of fatalities. At the end of the first pandemic wave, the duration of the supercritical phase was between two and three times longer when using the LSG protocol than when using the LFT protocol. The normalized number of fatalities was about 120 times higher in countries that applied the LSG protocol proposed by the Ferguson team at Imperial College [8] than in countries that applied the LFT protocol with mandatory contact tracing. The LSG protocol guarantees privacy, but the data show that it provides poor public health care since the number of COVID-19 fatalities is 120 times higher than that observed when employing the LFT protocol with mandatory mobile contact tracing.

4. Conclusions

In this work we extracted the time evolution of both the doubling time $T_d(t)$ and the success factor s by analyzing available data on the COVID-19 epidemic in seven countries that adopted different containment policies. The key result of this work is that we unveiled the presence two different regimes during the exponential growth of the positive case curve: (i) the stretched near threshold growth phase and (ii) the arrested phase. The two phases show two exponential functions of $T_d(t)$ versus time separated by a kink, characterized by two time exponents: s_1 and s_2. These success factors s are used to quantify the efficacy and success of the different mitigation methods. They could and should be used in the future to quickly and accurately monitor possible rebounds during this pandemic, but they are also valid for any future pandemic.

We clearly show that countries that adopted advanced technologies [13–15], i.e., the LFT containment policy with mandatory 'mobile contact tracing', were able to reduce both the peak and the width of the COVID-19 epidemic's daily positive case curve. The reduction in the duration of the lockdown obtained by mandatory 'contact tracing' minimized the impact on the economy [10] by keeping manufacturers closed for a shorter time. The number of fatalities per million people over 100 d, covering the full width of the first wave, was more than 100 times smaller than in the countries that did not use mandatory mobile contact tracing.

Finally, we showed that the time-dependent doubling time plots [13, 14, 31] for early warning on the epidemic spread rate gives reliable predictions, in particular during the early stage of spread. Therefore, the proposed method can be considered useful to predict the time evolution of future epidemics. This approach has a fundamental advantage over the standard analysis of the COVID-19 epidemic, and is in agreement with previous data analysis [12, 19]. In this study, based on data published on the 102nd DoY on the epidemic growth in Italy, France, Spain, the UK, and the USA, we predicted (see panel (c) in figure 3) the end of the positive case curve for each country (see table 1) within a couple of days. The results are validated in figure 4 and table 2, covering the first 100 d of the COVID-19 epidemic in different countries. Furthermore, all predictions were validated by data available on the 177th DoY, and a quantitative comparative evaluation of different protocols used for COVID-19 containment obtained. Finally, we hope that this original approach will help others understand the epidemiology of COVID-19 and help policymakers who are now well informed [31] save lives and reduce fatality numbers by two orders of magnitude in a second wave of COVID-19 or in a future pandemic.

Author contributions

The authors contributed equally to the conceptualization, methodology, and investigation while preparing the article.

Conflict of interest

The authors declare no conflicts of interest.

Acknowledgments

We acknowledge the non-profit organization *Superstripes-onlus* for funding this research.

ORCID iDs

Antonio Bianconi https://orcid.org/0000-0001-9795-3913
Augusto Marcelli https://orcid.org/0000-0002-8138-7547
Gaetano Campi https://orcid.org/0000-0001-9845-9394
Andrea Perali https://orcid.org/0000-0002-4914-4975

References

[1] National Health Commission of the People's Republic of China 2020 Update on the novel coronavirus pneumonia outbreak (http://nhc.gov.cn/xcs/yqtb/list_gzbd.shtml) (Accessed: 8 February 2020)
[2] World Health Organization 2020 Coronavirus disease (COVID-2019) situation reports (https://who.int/

emergencies/diseases/novel-coronavirus-2019/situation-reports/) (Accessed: 1 March 2020)
[3] Pueyo T 2020 Coronavirus: why you must act now (https://medium.com/@tomaspueyo/coronavirus-act-today-or-people-will-die-f4d3d9cd99ca) (Accessed: 12 March 2020)
[4] Hahn U, Chater N , Lagnado D *et al* Public request to take stronger measures of social distancing across the UK with immediate effect 2020 (https://vip.politicsmeanspolitics.com/2020/03/15/uk-scientists-on-coronavirus-open-letters-to-number-10/) (Accessed: 14 March 2020)
[5] Responding to Covid-19 with Tech 2020 (https://tech.gov.sg/) (Accessed: 9 April 2020)
[6] Maslov S and Goldenfeld N 2020 Window of opportunity for mitigation to prevent overflow of ICU capacity in Chicago by COVID-19 available at (https://medrxiv.org/content/10.1101/2020.03.20.20040048v1)
[7] Moghadas S M *et al* 2020 Projecting hospital utilization during the COVID-19 outbreaks in the United States *Proc. Natl Acad. Sci.* **117** 9122–6
[8] Ferguson N M *et al* 2020 Impact of non-pharmaceutical interventions (NPIs) to reduce COVID-19 mortality and healthcare demand *Report 19* Imperial College COVID-19 Response Team available online: (https://spiral.imperial.ac.uk:8443/handle/10044/1/77482)
[9] Lau M S Y, Cowling B J, Cook A R and Riley S 2015 Inferring influenza dynamics and control in households *Proc. Natl Acad. Sci.* **112** 9094–9
[10] Hatchett R J, Mecher C E and Lipsitch M 2007 Public health interventions and epidemic intensity during the 1918 influenza pandemic *Proc. Natl Acad. Sci.* **104** 7582–7
[11] Maier B F and Brockmann D 2020 Effective containment explains sub-exponential growth in confirmed cases of recent COVID-19 outbreak in Mainland China (arXiv:2002.07572)
[12] Ziff A L and Ziff R M 2020 Fractal kinetics of Covid-19 pandemics (medRxiv:10.1101/2020.02.16)
[13] Bianconi A, Marcelli A, Campi G and Perali A 2020 *Sul Controllo della Crescita della Diffusione della Pandemia Covid-19 e la Strategia delle Misure di Contenimento in Italia* (*Science Series*) (Rome: Superstripes Press) (https://superstripes.net/superstripes-press)
[14] Bianconi A, Marcelli A, Campi G and Perali A 2020 Ostwald growth rate in controlled Covid-19 epidemic spreading as in arrested growth in quantum complex matter *Condens. Matter* **5** 23
[15] Ferretti L, Wymant C, Kendall M, Zhao L, Nurtay A, Abeler-Dorner L, Parker M, Bonsall D and Fraser C 2020 Quantifying SARS-CoV-2 transmission suggests epidemic control with digital contact tracing *Science* **368** eabb6936
[16] Bnaya G, Zheng Z, Liu S, Chen X, Sela A, Li J, Li D and Havlin S 2020 Spatio-temporal propagation of COVID-19 pandemics (arXiv:2003.08382)
[17] Zlatic V, Barjasic I, Kadovic A, Stefancic H and Gabrielli A 2020 Bi-stability of SUDR + K model of epidemics and test kits applied to COVID-19 (arXiv:2003.08479)
[18] Liu Y, Sanhedrai H, Dong G, Shekhtman L M, Wang F, Buldyrev S V and Havlin S 2020 Efficient network immunization under limited knowledge (arXiv:2004.00825)
[19] Bianconi G and Krapivsky P L 2020 Epidemics with containment measures (arXiv:2004.03934)
[20] Wells C R *et al* 2020 Impact of international travel and border control measures on the global spread of the novel 2019 coronavirus outbreak *Proc. Natl. Acad. Sci.* **117** 7504–9
[21] Chinazzi M *et al* 2020 The effect of travel restrictions on the spread of the 2019 novel coronavirus (2019-nCoV) outbreak *Science* **368** 395–400
[22] Bray A J 2003 Coarsening dynamics of phase-separating systems *Phil. Trans. R. Soc.* A **361** 781–92
[23] Puri S and Wadhawan V 2009 *Kinetics of Phase Transitions* (Boca Raton, FL: CRC Press) p 153
[24] Ostwald W 1886 *Lehrbuch der Allgemeinen Chemie* (Leipzig: Wilhelm Engelmann)
[25] Poccia N, Fratini M, Ricci A, Campi G, Barba L, Vittorini-Orgeas A, Bianconi G, Aeppli G and Bianconi A 2011 Evolution and control of oxygen order in a cuprate superconductor *Nat. Mater.* **10** 733–6
[26] Poccia N *et al* 2012 Optimum inhomogeneity of local lattice distortions in La_2CuO_{4+y} *Proc. Natl. Acad. Sci.* **109** 15685–90
[27] Campi G *et al* 2015 Inhomogeneity of charge-density-wave order and quenched disorder in a high-T_c superconductor *Nature* **525** 359–62
[28] Chung S-Y, Kim Y-M, Kim J-G and Kim Y-J 2008 Multiphase transformation and Ostwald's rule of stages during crystallization of a metal phosphate *Nat. Phys.* **5** 68–73
[29] Streets A M and Quake S R 2010 Ostwald ripening of clusters during protein crystallization *Phys. Rev. Lett.* **104** 178102
[30] Campi G, Bianconi A, Perali A, Marcelli A and Valletta A 2020 The critical phase of Covid-19 epidemic in Italian regional outbreaks between the supercritical and subcritical phases (submitted)
[31] Bianconi A, Campi G, Marcelli A and Perali A 2020 Coronavirus, studiato il metodo fisico per il contenimento del virus L'Eurispes (https://leurispes.it/coronavirus-studiato-il-metodo-fisico-per-il-contenimento-del-virus/)